HHS Public Access

Author manuscript

Genes Brain Behav. Author manuscript; available in PMC 2018 November 01.

Published in final edited form as:

Genes Brain Behav. 2017 November ; 16(8): 745–755. doi:10.1111/gbb.12398.

ASIC1A in neurons is critical for fear-related behaviors

R. J. Taugher[1,2], **Y. Lu**[1,2], **R. Fan**[1,2], **A. Ghobbeh**[1,2], **C. J. Kreple**[3,4], **F. M. Faraci**[5,6], and **J. A. Wemmie**[1,2,3,4,7,8,9,10]

[1]Department of Psychiatry, University of Iowa, Iowa City, Iowa, USA

[2]Department of Veterans Affairs Medical Center, Iowa City, Iowa, USA

[3]Medical Scientist Training Program, University of Iowa, Iowa City, Iowa, USA

[4]Department of Molecular Physiology and Biophysics, University of Iowa, Iowa City, Iowa, USA

[5]Department of Internal Medicine, University of Iowa, Iowa City, Iowa, USA

[6]Department of Pharmacology, University of Iowa, Iowa City, Iowa, USA

[7]Department of Neurosurgery, University of Iowa, Iowa City, Iowa, USA

[8]Pappajohn Biomedical Institute, University of Iowa, Iowa City, Iowa, USA

[9]Interdisciplinary Graduate Program in Neuroscience, University of Iowa, Iowa City, Iowa, USA

[10]Roy J. Carver Chair of Psychiatry and Neuroscience

Abstract

Acid-sensing ion channels (ASICs) have been implicated in fear-, addiction-, and depression-related behaviors in mice. While these effects have been attributed to ASIC1A in neurons, it has been reported that ASICs may also function in non-neuronal cells. To determine if ASIC1A in neurons is indeed required, we generated neuron-specific knockout mice with floxed *Asic1a* alleles disrupted by Cre recombinase driven by the neuron-specific synapsin I promoter (*SynAsic1a KO mice)*. We confirmed that Cre expression occurred in neurons, but not all neurons, and not in non-neuronal cells including astrocytes. Consequent loss of ASIC1A in some but not all neurons was verified by western blotting, immunohistochemistry, and electrophysiology. We found ASIC1A was disrupted in fear circuit neurons, and *SynAsic1a KO* mice exhibited prominent deficits in multiple fear-related behaviors including Pavlovian fear conditioning to cue and context, predator odor-evoked freezing, and freezing responses to carbon dioxide inhalation. In contrast, in the nucleus accumbens ASIC1A expression was relatively normal in *SynAsic1a KO* mice, and consistent with this observation, cocaine conditioned place preference (CPP) was normal. Interestingly, depression-related behavior in the forced swim test, which has been previously linked to ASIC1A in the amygdala, was also normal. Together, these data suggest neurons are an important site of ASIC1A action in fear-related behaviors, whereas other behaviors likely depend on ASIC1A in other neurons or cell types not targeted in *SynAsic1a KO* mice.

Address Correspondence to: John A. Wemmie MD PhD, Roy J. and Lucille A. Carver College of Medicine, University of Iowa, Iowa City, IA 52242, Phone: 319-384-3173, Fax: 319-384-3176, john-wemmie@uiowa.edu.

Conflict of Interest: The authors declare no competing financial interests.

These findings highlight the need for further work to discern the roles of ASICs in specific cell types and brain sites.

Keywords

ASIC1A; neurons; anxiety; fear; pH

Introduction

A wide variety of behaviors, including behaviors related to fear, depression, and addiction, share a surprising dependence on a family of ion channels that are activated by acid. These channels, acid-sensing ion channels (ASICs), are trimeric, proton-gated cation channels of the degenerin/epithelial sodium channel (DEG/ENaC) family that are expressed throughout the nervous system and are activated by reduction in extracellular pH (Waldmann et al., 1997, Jasti et al., 2007, Wemmie et al., 2003, Wemmie et al., 2013, Zha, 2013). Acid-sensing ion channel-1A (ASIC1A) is a critical channel subunit, as genetic disruption or pharmacological inhibition of ASIC1A largely abolishes currents in brain neurons evoked by acidosis in the physiological range (Wemmie et al., 2002, Xiong et al., 2004, Wu et al., 2013). Beyond their pH sensitivity, the role that these channels play in behavior remains poorly understood. To elucidate this role, it is first important to identify the brain areas and cell types in which the channels function to influence behavior.

Though ASIC1A expression occurs throughout the brain, its expression is particularly abundant in brain structures underlying emotive behaviors, such as the amygdala, bed nucleus of the stria terminalis (BNST), periaqueductal gray (PAG), dorsal striatum, and nucleus accumbens (NAc) (Wemmie et al., 2003, Zhang et al., 2009, Taugher et al., 2014, Kreple et al., 2014, Price et al., 2014). Consistent with expression in these brain areas, knocking out the *Asic1a* gene in mice results in an array of phenotypes in behavioral assays including cued and contextual fear conditioning, unconditioned freezing to carbon dioxide (CO_2) and the predator odor trimethylthiazoline (TMT), depression-related behaviors including the forced swim test, and addiction-related behaviors such as cocaine conditioned place preference (CPP), and cocaine-induced locomotion (Coryell et al., 2007, Price et al., 2014, Wemmie et al., 2003, Ziemann et al., 2009, Coryell et al., 2009, Taugher et al., 2014, Taugher et al., 2015, Kreple et al., 2014, Jiang et al., 2013). Region-restricted manipulations of ASIC1A in the amygdala, NAc, and BNST further implicate these brain areas as sites of ASIC1A action in behavior (Ziemann et al., 2009, Coryell et al., 2009, Taugher et al., 2014, Taugher et al., 2015, Kreple et al., 2014, Coryell et al., 2008, Chiang et al., 2015).

Despite these established behavioral phenotypes, it remains unclear in which cell types ASIC1A exerts its effects. ASIC1A is expressed in neurons and has been located in the soma, axons, dendrites, and dendritic spines, where it has been implicated in synaptic transmission and plasticity (Wemmie et al., 2002, Zha et al., 2006, Zha et al., 2009, Du et al., 2014, Kreple et al., 2014). However, recent studies have suggested that ASICs might also be present in subpopulations of glial cells (Huang et al., 2010, Feldman et al., 2008, Lin et al., 2010, Yang et al., 2016) and may contribute to acid-evoked currents and calcium influx in

astrocytes (Huang et al., 2010, Yang et al., 2016), although relative levels of ASIC1A expression in neurons and non-neuronal cells remain unclear. Most of the tools previously used to manipulate ASIC1A have not discriminated between neuronal and non-neuronal cells. One study used Tg(Nestin-cre) mice with the goal of disrupting *Asic1a* specifically in neurons and found a reduction in both cued and contextual fear conditioning (Chiang et al., 2015). However, because Tg(Nestin-cre) mice express Cre in both neuronal and non-neuronal cells (Harno et al., 2013, Walker et al., 2010), it remains an open question in which cell types ASIC1A acts to exert its effect on behavior. Thus, we sought to test the hypothesis that neurons are a key site of ASIC1A action in emotive behaviors.

Materials and Methods

Mice

Asic1a$^{-/-}$ and *Asic1a*$^{loxP/loxP}$ mice were generated as previously described (Wemmie et al., 2002, Taugher et al., 2014, Kreple et al., 2014). Tg(Syn1-cre) mice (Zhu et al., 2001) were obtained from Dr. Curt Sigmund. Tg(Syn1-cre) and *Asic1a*$^{loxP/loxP}$ mice were intercrossed to generate *Asic1a*$^{loxP/loxP}$ Tg(Syn1-cre) mice, herein referred to *SynAsic1a KO* mice. Because of previously reported expression of Cre in germline cells (Rempe et al., 2006), all offspring were screened for excision of the *Asic1a* floxed allele in non-neuronal tissue. *Gt(ROSA)26Sor*$^{tm6(CAG-ZsGreen1)Hz}$ Cre reporter mice, purchased from the Jackson Laboratory (stock no. 007906) (Madisen et al., 2010), were intercrossed with Tg(Syn1-cre) mice to produce Gt(ROSA)26Sor$^{tm6(CAG-ZsGreen1)Hz}$ Tg(Syn1-cre) mice, referred to as *SynRosa26* mice. *Asic1a*$^{-/-}$ and *SynRosa26* mice were maintained on a congenic C57BL/6J background, whereas the *SynAsic1a KO* mice were on a mixed C57BL/6J and C57BL/6T background. All mice had ad libitum access to water and standard chow, and were group housed. Mice were kept on a 12-hour light-dark cycle and all experiments were performed during the light cycle. Mice of both sexes were used and all experimental groups were sex- and age-matched (10–16 weeks of age). Naïve mice were used for immunohistochemistry, western blotting, and electrophysiology. Mice underwent testing in multiple behaviors in the following order: open field, TMT-evoked freezing, CO_2-evoked freezing, forced swim test, and fear conditioning, with at least 24hrs between asssays. A separate cohort of mice was used to test cocaine conditioned place preference. Animal care met the standards set by the National Institutes of Health, and all experiments were approved by the University of Iowa Animal Care and Use Committee.

Immunohistochemistry and Imaging

eGFP expression in slices from *SynRosa26* mice was directly imaged without use of antibodies. Immunohistochemistry was performed as previously described (Taugher et al., 2014). Briefly, rabbit polyclonal anti-ASIC1 antiserum (MTY19) (Wemmie et al., 2003) diluted 1:1000 was used for ASIC1A immunohistochemistry, a mouse monoclonal NeuN antibody (Millipore) diluted 1:250 was used to identify neuronal nuclei, and a mouse monoclonal GFAP antibody (Millipore) diluted 1:500 was used to identify astrocytes. Secondary antibodies included goat-anti rabbit IgG antibody coupled to Alexa Fluor 488 (Invitrogen) for ASIC1A immunohistochemistry, and goat-anti mouse IgG antibody coupled

to Alexa Fluor 568 (Invitrogen) for NeuN and GFAP staining. All sections were imaged at 10× with a confocal microscope (Zeiss 710).

DNA Isolation and PCR

DNA was isolated from tail and brain tissue using the QiAamp DNA Mini Kit (Qiagen). PCR primers were used to identify the presence or excision of the *Asic1a* floxed allele. Primer sequences were as follows (5' to 3'): forward primer: GAGAACTGGAGACACAGAAGGTGAGGA, reverse primer: GCCTGACACATGGAATACAAGAAGACA.

Western blotting

Brain lysates were prepared and western blotting was performed as previously described (Taugher et al., 2014). Briefly, the primary antibodies were: rabbit polyclonal anti-ASIC1 antiserum (MTY19)(Wemmie et al., 2003) diluted 1:500 and chicken polyclonal anti-GAPDH antibody (Millipore) diluted 1:10000. The secondary antibodies were: IRDye 800CW Donkey anti-Rabbit IgG and IRDye 680LT Donkey anti-Chicken IgG (LI-COR) (1:10000). The membrane was imaged with the Odyssey imaging system (LI-COR).

Slice electrophysiology

Coronal slices through the amygdala and NAc (300 μm) were prepared from 8–12 week old mice and whole-cell recordings were performed as previously described (Taugher et al., 2014).

Fear conditioning

A 3-day protocol was used to assess both cued and contextual fear conditioning. On the first day, mice were placed in a near-infrared video fear conditioning chamber (Med Associates). After 3 minutes, a 20-second tone (90 db) was played which co-terminated with a 1-second footshock (0.75 mA.) Four more tone-shock pairings were delivered with an 80-second inter-stimulus interval. On the second day, cue-evoked responses were tested in a novel context in which lighting, floor texture, and odor had been altered. After three minutes in the novel context, mice were exposed to a 3-minute tone (90db), followed by an additional 4 minutes without the tone. On the third day, contextual fear memory was tested by returning the mice to the original training context for five minutes. Freezing and maximum motion following footshock were scored with VideoFreeze software (Med Associates).

TMT-evoked freezing

TMT-evoked freezing was performed as previously described (Taugher et al., 2015). Briefly, mice were placed in a Plexiglas behavior chamber along with a beaker containing a piece of tissue paper soaked with 6 μL trimethylthiazoline (TMT) (Contech enterprises) for 10 minutes. Mice were videotaped and freezing and time exploring the beaker were scored by a trained observer, blinded to genotype. Freezing was defined as an absence of motion other than respiration. Exploring the beaker was defined as sniffing, touching, or climbing on the beaker.

CO_2-evoked freezing

CO_2-evoked freezing was assessed as previously described (Taugher et al., 2014, Price et al., 2014, Ziemann et al., 2009). In brief, mice were placed in a plexiglas chamber that was continuously infused with 10% CO_2 (10% CO_2, 21% O_2, balanced with N_2) at a rate of 5L/minute for 10 minutes. Mice were videotaped and freezing behavior was scored by a trained observer, blinded to genotype. Freezing was defined as the absence of motion other than respiration.

Forced swim test

The forced swim test was assessed as previously described (Coryell et al., 2009). Mice were placed in a 4L plastic beaker filled with approximately 3.5L of room temperature water for 6 minutes. Mice were videotaped and immobility was scored by a trained observer, blinded to genotype. Immobility was defined as an absence of motion except for gliding and small movements required to keep the head above water.

Cocaine conditioned place preference

Cocaine conditioned place preference was performed using a five-day protocol with counterbalanced conditions as previously described (Kreple et al., 2014), using cocaine (10 mg/kg, diluted in 0.9% saline, i.p., 10 μl/g body mass, Sigma Aldrich) and saline (10 μl/g body mass). Time spent on each side of the chamber during pretest and posttest was quantified by a trained observer blinded to genotype. To ensure that none of the mice had a strong inherent place preference, we screened the pretest data to ensure that no mouse spent more than 75% of the time on either side of the chamber during the pretest. None of the mice met this criterion, thus all mice were included in the subsequent analysis. Conditioned place preference was assessed by subtracting the time spent on the cocaine paired side during the pretest from that during the posttest.

Statistical analysis

All values are reported and plotted as mean ± SEM. A Student's t-test was used to test significance between two groups; Welch's correction was applied when comparsions were made between groups with unequal variance. Where appropriate, the Holm-Sidak method was used to correct for multiple comparisons. A Fisher's exact test was used to compare two proportions. $p < 0.05$ was considered significant for all tests. A Grubb's test (Alpha = 0.05) was used to identify outliers. Two outliers were identified in the TMT-evoked freezing assay (1 *Asic1a*$^{+/+}$ mouse and 1 *SynAsic1a KO* mouse), and excluded from further analysis. Sample sizes vary between experiments and are stated in the figure legends. All analyses were performed using Prism software (GraphPad).

Results

Cre expression in Tg(Syn1-cre) mice is neuron-specific

We first sought to verify that the Tg(Syn1-cre) mice express Cre specifically in neurons. To characterize the location of Cre expression, we crossed the Tg(Syn1-cre) mice with *Gt(ROSA)26Sor*$^{tm6(CAG-ZsGreen1)Hz}$ reporter mice, which express eGFP in Cre-positive

cells. Confocal imaging of the offspring, referred to as *SynRosa26* mice, revealed widespread Cre expression throughout the brain, including the amygdala, BNST, cortex, hippocampus, hypothalamus, lateral septum, olfactory bulb, and thalamus (Figure 1A–1B, Figure S1A–S1D). However, other areas such as the striatum, had relatively fewer Cre-positive cells (Figure 1A–1B). To assess whether or not Cre was expressed specifically in neurons, we looked at the colocalization of the Cre-positive cells with NeuN, a marker of neuronal nuclei. We found that all visible Cre-positive cells in the amygdala colocalized with NeuN, however some NeuN expressing cells were Cre-negative (Figure 1C). These observations suggest that Cre expression in the Tg(Syn1-cre) mice is specific to neurons, although not all neurons expressed Cre. We also examined co-localization of Cre with GFAP, an astrocyte marker. Cre-positive puncta did not colocalize with GFAP or the small blood vessels surrounded by GFAP expressing astrocytes (Figure 1D), suggesting that Cre was not expressed in astrocytes or small vessels, and consistent with the observation that Cre expression was neuron specific.

Disruption of *Asic1a* allele and ASIC1A protein in *SynAsic1a KO* mice

Next we crossed Tg(Syn1-cre) mice to *Asic1a* $^{loxP/loxP}$ mice to produce targeted disruption of ASIC1A in Cre-expressing neurons, referred to as *SynAsic1a KO* mice. To confirm disruption of *Asic1a*, we analyzed DNA isolated from the tail and brain by PCR. We found that the *Asic1a* floxed allele was present in an unexcised state in tail DNA from *SynAsic1a KO* mice, but was detected in both excised and unexcised states in DNA samples from whole brain lysates (Figure S2A–S2C), suggesting that Cre was not expressed in tail, but was expressed in some, but not all brain cells. We next tested ASIC1A protein in brain. Western blotting whole brain lysates revealed a decrease in ASIC1A protein in *SynAsic1a KO* mice, relative to Cre-negative *Asic1a*$^{loxP/loxP}$ littermate controls ($t(6) = 8.683$, ***$p = 0.0001$), but it was not absent in the *SynAsic1a KO* mice like in the *Asic1a*$^{-/-}$ mice (Figure 2A, Figure S3A). A partial disruption of ASIC1A was similarly observed in amygdala lysates (Figure 2B, Figure S3B). Likewise, ASIC1A immunohistochemistry also suggested an incomplete loss of ASIC1A protein in the amygdala and BNST of *SynAsic1a KO* mice compared to littermate controls (Figure 2C).

We also assessed acid-evoked current in BLA neurons. Although ASIC1A-dependent currents can be evoked in BLA neurons by relatively small reductions in extracellular pH (Ziemann et al., 2009), we have previously found that an extreme acid challenge (e.g. pH 5 to 5.6) evokes maximal or near maximal currents in essentially all BLA neurons, and that global disruption of ASIC1A in *Asic1a*$^{-/-}$ mice eliminates these currents (Wemmie et al., 2003, Ziemann et al., 2009). Thus, the presence or absence response to pH 5.6 provides a useful surrogate for assessing presence or absence of ASIC1A protein on the cell surface of individual neurons. In control *Asic1a*$^{loxP/loxP}$ mice, we found pH 5.6 evoked current in all of the BLA neurons tested, whereas in the *SynAsic1a KO* mice, more than half of the neurons tested lacked acid-evoked currents (Fisher's exact, **$p = 0.0031$) (Figure 2D–2E). The neurons that retained acid-evoked current in the *SynAsic1a KO* mice exhibited normal current density ($t(17) = 0.2786$, $p = 0.7839$) (Figure 2F). Together, these findings suggest that ASIC1A is reduced, though not completely eliminated in the *SynAsic1a KO* brain and

that the loss of ASIC1A was due to excision of the floxed alleles in a subset of neurons, whereas other neurons retained normal levels of ASIC1A expression.

Conditioned and unconditioned fear-related behaviors are reduced in *SynAsic1a KO* mice

We next sought to test the behavioral effects of ASIC1A disruption in the *SynAsic1a KO* mice. We tested *SynAsic1a KO* mice versus Cre negative $Asic1a^{loxP/loxP}$ littermates. For direct comparison we also simultaneously retested the effects of global disruption of ASIC1A by comparing $Asic1a^{-/-}$ mice versus $Asic1a^{+/+}$ controls. We assessed conditioned fear using a combined cued and contextual fear conditioning paradigm, and found that the *SynAsic1a KO* mice exhibited reduced freezing during acquisition ($Asic1a^{-/-}$, t(18) = 4.355, ***p = 0.0004; *SynAsic1a KO*, t(29) = 5.061, ***p < 0.0001), cued testing ($Asic1a^{-/-}$, t(18) = 3.25, **p = 0.0044; *SynAsic1a KO*, t(29) = 6.008, ***p < 0.0001), and context testing ($Asic1a^{-/-}$, t(18) = 2.322, *p = 0.0321; *SynAsic1a KO*, t(28) = 4.963, ***p < 0.0001) relative to Cre negative $Asic1a^{loxP/loxP}$ controls (Figure 3A, Figure S4A–S4B). Furthermore, the deficits in the *SynAsic1a KO* mice were similar to the deficits in the $Asic1a^{-/-}$ mice lacking ASIC1A globally. Although freezing was reduced, unconditioned responses to the footshock were intact in the *SynAsic1a KO* mice (t(17) = 0.8263, p = 0.4201) and increased in the $Asic1a^{-/-}$ mice (t(12.03) = 2.41, *p = 0.0329), suggesting that these mice do perceive the footshock (Figure S4C). In addition, like the $Asic1a^{-/-}$ mice, the *SynAsic1a KO* mice exhibited abnormally low freezing in response to 10% CO_2 ($Asic1a^{-/-}$, t(19) = 3.181, **p = 0.0049; *SynAsic1a KO*, t(29) = 4.365, ***p = 0.0001) as well as to TMT($Asic1a^{-/-}$, t(18) = 3.712, **p = 0.0016; *SynAsic1a KO*, t(28) = 4.888, ***p < 0.0001) (Figure 3B–3C). Consistent with this reduction in freezing, the $Asic1a^{-/-}$ mice and the *SynAsic1a KO* mice, avoidance of the TMT−containing beaker was also reduced ($Asic1a^{-/-}$, t(10.07) = 2.512, *p = 0.0306; *SynAsic1a KO*, t(16.65) = 2.757, *p = 0.0136) (Figure S5). Together, these observations suggest that ASIC1A in neurons, likely in the fear circuit, is critical for multiple fear-related behaviors.

To control for locomotor activity, we also assessed locomotion in the open field. Locomotor activity was similar between *SynAsic1a KO* and $Asic1a^{loxP/loxP}$ control mice (data not shown, p = 0.7442), which was consistent with the previous observation that locomotor activity did not differ between $Asic1a^{-/-}$ mice and $Asic1a^{+/+}$controls (Coryell et al., 2007).

SynAsic1a KO mice express ASIC1A in the NAc

In contrast to Cre expression and Cre-mediated disruption of ASIC1A in the amygdala and BNST, Cre was not expressed uniformly throughout the brain in the *SynRosa26* mice. Relatively little Cre expression was observed in striatal structures such as the NAc (Figures 1A, 1B and 4A). Likewise, western blotting and immunohistochemistry revealed only slightly reduced ASIC1A protein levels in the NAc in *SynAsic1a KO* mice (Figure 4B–4C, Figure S3C). Similarly, although we found some neurons in the NAc from *SynAsic1a KO* mice that lacked acid-evoked currents, most did exhibit acid-evoked current, suggesting that *Asic1a* was disrupted in relatively few NAc neurons (Fisher's exact, p = 0.2228) (Figure 4D–4E). The *SynAsic1a KO* neurons that retained acid-evoked currents displayed current densities that were not statistically different from controls, although they tended to be lower (t(13.83) = 2.155, p = 0.0530) (Figure 4F). Together these data suggest that Cre was

expressed in relatively few neurons in the NAc and striatum, and thus ASIC1A expression was largely retained. This result was somewhat surprising because the synapsin 1 promotor has often been considered pan neuronal and the endogenous synapsin promoter produces widespread transcription in the brain, including the striatum (Lein et al., 2007). However, inconsistent levels of gene expression across brain sites have been seen with other transgenic mice including mice with other transgenes driven by the synapsin 1 promoter (Wemmie, 2004). This variability is likely due to location differences between genomic sites of transgene integration. Nevertheless, the relative sparing of ASIC1A expression in some brain areas provided an opportunity to test whether ASIC1A may affect different behaviors through different sites of action.

NAc dependent behavior is intact in *SynAsic1a KO* mice

The NAc plays important roles in addiction-related behavior and plasticity (Russo et al., 2010), and our previous work demonstrated that ASIC1A in the NAc was necessary and sufficient for normal cocaine CPP (Kreple et al., 2014). Therefore we tested if the residual ASIC1A expression, in the NAc and possibly elsewhere, in the *SynAsic1a KO* mice was sufficient to maintain normal cocaine CPP. Indeed, we found no significant differences in cocaine CPP between the *SynAsic1a KO* mice and Cre-negative $Asic1a^{loxP/loxP}$control mice ($Asic1a^{-/-}$, t(26) = 2.502, *p = 0.0190; *SynAsic1a KO*, t(18) = 0.003232, p = 0.9975) (Figure 5A), whereas the previously described increase in cocaine CPP in the $Asic1a^{-/-}$ mice was reproduced.

Normal forced swim behavior in *SynAsic1a KO* mice

Previous work found that $Asic1a^{-/-}$ mice have reduced depression-related behaviors in several assays, including the forced swim test (Coryell et al., 2009). That work further suggested a critical role for ASIC1A in the amygdala (Coryell et al., 2009). Because the *SynAsic1a KO* mice have substantially reduced ASIC1A expression in the amygdala, we hypothesized that they may also exhibit reduced depression-related behavior. However, contrary to our hypothesis, the *SynAsic1a KO* mice had similar levels of immobility in the forced swim test relative to littermate Cre-negative $Asic1a^{loxP/loxP}$ controls ($Asic1a^{-/-}$, t(18) = 2.428, *p = 0.0259; *SynAsic1a KO*, t(29) = 1.648, p = 0.1101) (Figure 5B). Moreover, because fear conditioning and other fear-related behaviors were severely disrupted in the *SynAsic1a KO* mice, these results suggest that the site(s) of action of ASIC1A in forced swim behavior likely differs from these other fear-related behaviors. To our knowledge this is the first evidence that the mechanisms underlying ASIC1A action in depression-related behavior may be separable from those underlying fear-related behavior.

Discussion

The primary impact of this work is in its investigation of the cellular site of ASIC1A action in emotive behaviors. In *SynAsic1a KO* mice, Cre-mediated disruption of ASIC1A was restricted to neurons, although not all neurons were affected. Therefore, the observation that *SynAsic1a KO* mice exhibit deficits similar to $Asic1a^{-/-}$ mice in fear conditioning, TMT-evoked freezing, and CO_2-evoked freezing (Figure 3A–C) suggests a neuronal site of ASIC1A action, at least in these behaviors.

While our experiments reproduced the effects of global *Asic1a*$^{-/-}$ disruption, the *SynAsic1a KO* mice did not exhibit all of the behavioral phenotypes detected in global *Asic1a*$^{-/-}$ mice. Some of the behaviors tested here, namely cocaine CPP and forced swim behavior, did not differ from controls expressing normal ASIC1A levels. One possible explanation is the difference in genetic background between the *SynAsic1a KO* and *Asic1a*$^{-/-}$ mice. Alternatively, the ASIC1A expression that was retained in the *SynAsic1a KO* mice, might be sufficiently preserved at some key location(s) to maintain the unaffected behaviors. Unfortunately, the present studies do not allow us to discern whether these locations might be non-neuronal cells or Cre-negative neurons. Our previous work found that virus-mediated expression of ASIC1A in the NAc of *Asic1a*$^{-/-}$ mice was sufficient to normalize cocaine CPP (Kreple et al., 2014), thus the residual ASIC1A expression in the NAc of the *SynAsic1a KO* mice might explain their normal CPP behavior. However, because this virus-mediated restoration of ASIC1A in the NAc was not cell-type specific, the possibility that ASIC1A in non-neuronal cells might contribute to cocaine CPP cannot be excluded.

The site of ASIC1A action in the forced swim test also remains unclear. Previous work found that virus-mediated expression of ASIC1A in the amygdala in global *Asic1a*$^{-/-}$ mice was sufficient to normalize immobility (Coryell et al., 2009). Thus we were surprised that, despite the substantial reduction of ASIC1A expression in the amygdala, the *SynAsic1a KO* mice exhibited normal behavior in the forced swim test. Perhaps the residual ASIC1A expression in the amygdala was sufficient to maintain forced swim behavior in the *SynAsic1a KO* mice. Alternatively, ASIC1A in the amygdala may not be necessary for normal forced swim behavior. Conceivably, ASIC1A at other, possibly redundant sites may be sufficient. Potential candidate sites include the NAc and the dorsal striatum, because ASIC1A expression was relatively preserved in these locations in *SynAsic1a KO* mice and these regions have also been implicated in the forced swim test (Rada et al., 2003, Colelli et al., 2014)

Although our results suggest an important role for ASIC1A in neurons in fear-related behavior, there remains the question of how ASIC1A affects neuronal function. One possibility is that ASIC1A responds to acidosis at synapses during synaptic transmission. Consistent with this possibility, recent work identified an ASIC1A-dependent postsynaptic current which was sensititve to extracellular pH buffering capacity as well as to genetic disruption and pharmacologic inhibitition of carbonic anhydrase (Kreple et al., 2014, Du et al., 2014, Gonzalez-Inchauspe et al., 2017). Alternatively, the observed behavioral effects may result more directly from the remodeling of dendritic spines that has been observed following the loss of ASIC1A, for example in the hippocampus and NAc (Zha et al., 2006, Kreple et al., 2014). Moreover, the expression of ASIC1A in multiple brain regions and neuron types raises questions about whether it acts in similar or different ways in distinct populations of neurons. Clearly, more work is needed to better understand the mechanisms by which ASIC1A influences behavior and neuron physiology.

Results and their interpretations are limited by the experimental tools used to obtain them. While we were unable to detect Cre expression outside of neurons (Figure 1C) it is difficult to exclude Cre expression in all non-neuronal cells in the *SynAsic1a KO* mice. Similarly, we cannot rule out the possibility that the behavioral phenotypes seen in the *SynAsic1a KO*

mice are due to a loss of ASIC1A during development. However, previous studies suggest that the behavioral phenotypes observed here do not depend on developmental effects of ASIC1A, because disrupting *Asic1a* after development in adult animals recapitulated findings in global *Asic1a*$^{-/-}$ mice (Taugher et al., 2014, Kreple et al., 2014, Taugher et al., 2015).

While our results are consistent with an important role for ASIC1A in neurons, the potential role(s) of ASIC1A in non-neuronal cells is unclear. Ultimately, understanding where and how ASIC1A functions will be critical for fully understanding the biology of these channels and their unique properties. This knowledge will be of value for learning to leverage ASICs for thereapeutic purposes for illnesses such as anxiety, depression, and drug abuse.

Supplementary Material

Refer to Web version on PubMed Central for supplementary material.

Acknowledgments

J.A.W. was supported by the Department of Veterans Affairs (Merit Award), the NIMH (5R01MH085724), NHLBI (R01HL113863) and a NARSAD Independent Investigator Award and the Carver Foundation. F.M.F. was supported by the Department of Veterans Affairs (Merit Award), the NHLBI (R01HL113863) and the Fondation Leduq. R.J.T. was supported by NIMH training grant T32MH019113. C.J.K. was supported by NINDS training grant T32NS045549. We thank Dr. Curt Sigmund for providing us with the Tg(Syn1-cre) mice. We also thank Yimo Wang and the University of Iowa Central Microscopy Facility (1 S10 RR025439-01) for their assistance.

References

CHIANG PH, CHIEN TC, CHEN CC, YANAGAWA Y, LIEN CC. ASIC-dependent LTP at multiple glutamatergic synapses in amygdala network is required for fear memory. Sci Rep. 2015; 5:10143. [PubMed: 25988357]

COLELLI V, CAMPUS P, CONVERSI D, ORSINI C, CABIB S. Either the dorsal hippocampus or the dorsolateral striatum is selectively involved in consolidation of forced swim-induced immobility depending on genetic background. Neurobiol Learn Mem. 2014; 111:49–55. [PubMed: 24667495]

CORYELL M, ZIEMANN AE, WESTMORELAND PJ, HAENFLER JM, KURJAKOVIC Z, ZHA XM, PRICE M, SCHNIZLER MK, WEMMIE J. Targeting ASIC1a reduces innate fear and alters neuronal activity in the fear circuit. Biol Psychiatry. 2007; 62:1140–1148. [PubMed: 17662962]

CORYELL MW, WUNSCH AM, HAENFLER JM, ALLEN JE, MCBRIDE JL, DAVIDSON BL, WEMMIE JA. Restoring Acid-sensing ion channel-1a in the amygdala of knock-out mice rescues fear memory but not unconditioned fear responses. J Neurosci. 2008; 28:13738–41. [PubMed: 19091964]

CORYELL MW, WUNSCH AM, HAENFLER JM, ALLEN JE, SCHNIZLER M, ZIEMANN AE, COOK MN, DUNNING JP, PRICE MP, RAINIER JD, LIU Z, LIGHT AR, LANGBEHN DR, WEMMIE JA. Acid-sensing ion channel-1a in the amygdala, a novel therapeutic target in depression-related behavior. J Neurosci. 2009; 29:5381–8. [PubMed: 19403806]

DU J, REZNIKOV LR, PRICE MP, ZHA XM, LU Y, MONINGER TO, WEMMIE JA, WELSH MJ. Protons are a neurotransmitter that regulates synaptic plasticity in the lateral amygdala. Proc Natl Acad Sci U S A. 2014; 111:8961–6. [PubMed: 24889629]

FELDMAN DH, HORIUCHI M, KEACHIE K, MCCAULEY E, BANNERMAN P, ITOH A, ITOH T, PLEASURE D. Characterization of acid-sensing ion channel expression in oligodendrocyte-lineage cells. Glia. 2008; 56:1238–49. [PubMed: 18452213]

GONZALEZ-INCHAUSPE C, URBANO FJ, DI GUILMI MN, UCHITEL OD. Acid-Sensing Ion Channels Activated by Evoked Released Protons Modulate Synaptic Transmission at the Mouse Calyx of Held Synapse. J Neurosci. 2017; 37:2589–2599. [PubMed: 28159907]

HARNO E, COTTRELL EC, WHITE A. Metabolic pitfalls of CNS Cre-based technology. Cell Metab. 2013; 18:21–8. [PubMed: 23823475]

HUANG C, HU ZL, WU WN, YU DF, XIONG QJ, SONG JR, SHU Q, FU H, WANG F, CHEN JG. Existence and distinction of acid-evoked currents in rat astrocytes. Glia. 2010; 58:1415–24. [PubMed: 20549751]

JASTI J, FURUKAWA H, GONZALES EB, GOUAUX E. Structure of acid-sensing ion channel 1 at 1.9 A resolution and low pH. Nature. 2007; 449:316–323. [PubMed: 17882215]

JIANG Q, WANG CM, FIBUCH EE, WANG JQ, CHU XP. Differential regulation of locomotor activity to acute and chronic cocaine administration by acid-sensing ion channel 1a and 2 in adult mice. Neuroscience. 2013; 246:170–8. [PubMed: 23644053]

KREPLE CJ, LU Y, TAUGHER RJ, SCHWAGER-GUTMAN AL, DU J, STUMP M, WANG Y, GHOBBEH A, FAN R, COSME CV, SOWERS LP, WELSH MJ, RADLEY JJ, LALUMIERE RT, WEMMIE JA. Acid-sensing ion channels contribute to synaptic transmission and inhibit cocaine-evoked plasticity. Nat Neurosci. 2014; 17:1083–91. [PubMed: 24952644]

LEIN ES, HAWRYLYCZ MJ, AO N, AYRES M, BENSINGER A, BERNARD A, BOE AF, BOGUSKI MS, BROCKWAY KS, BYRNES EJ, CHEN L, CHEN L, CHEN TM, CHIN MC, CHONG J, CROOK BE, CZAPLINSKA A, DANG CN, DATTA S, DEE NR, DESAKI AL, DESTA T, DIEP E, DOLBEARE TA, DONELAN MJ, DONG HW, DOUGHERTY JG, DUNCAN BJ, EBBERT AJ, EICHELE G, ESTIN LK, FABER C, FACER BA, FIELDS R, FISCHER SR, FLISS TP, FRENSLEY C, GATES SN, GLATTFELDER KJ, HALVERSON KR, HART MR, HOHMANN JG, HOWELL MP, JEUNG DP, JOHNSON RA, KARR PT, KAWAL R, KIDNEY JM, KNAPIK RH, KUAN CL, LAKE JH, LARAMEE AR, LARSEN KD, LAU C, LEMON TA, LIANG AJ, LIU Y, LUONG LT, MICHAELS J, MORGAN JJ, MORGAN RJ, MORTRUD MT, MOSQUEDA NF, NG LL, NG R, ORTA GJ, OVERLY CC, PAK TH, PARRY SE, PATHAK SD, PEARSON OC, PUCHALSKI RB, RILEY ZL, ROCKETT HR, ROWLAND SA, ROYALL JJ, RUIZ MJ, SARNO NR, SCHAFFNIT K, SHAPOVALOVA NV, SIVISAY T, SLAUGHTERBECK CR, SMITH SC, SMITH KA, SMITH BI, SODT AJ, STEWART NN, STUMPF KR, SUNKIN SM, SUTRAM M, TAM A, TEEMER CD, THALLER C, THOMPSON CL, VARNAM LR, VISEL A, WHITLOCK RM, WOHNOUTKA PE, WOLKEY CK, WONG VY, WOOD M, YAYLAOGLU MB, YOUNG RC, YOUNGSTROM BL, YUAN XF, ZHANG B, ZWINGMAN TA, JONES AR. Genome-wide atlas of gene expression in the adult mouse brain. Nature. 2007; 445:168–76. [PubMed: 17151600]

LIN YC, LIU YC, HUANG YY, LIEN CC. High-density expression of Ca2+-permeable ASIC1a channels in NG2 glia of rat hippocampus. PLoS One. 2010:5.

MADISEN L, ZWINGMAN TA, SUNKIN SM, OH SW, ZARIWALA HA, GU H, NG LL, PALMITER RD, HAWRYLYCZ MJ, JONES AR, LEIN ES, ZENG H. A robust and high-throughput Cre reporting and characterization system for the whole mouse brain. Nat Neurosci. 2010; 13:133–40. [PubMed: 20023653]

PRICE MP, GONG H, PARSONS MG, KUNDERT JR, REZNIKOV LR, BERNARDINELLI L, CHALONER K, BUCHANAN GF, WEMMIE JA, RICHERSON GB, CASSELL MD, WELSH MJ. Localization and behaviors in null mice suggest that ASIC1 and ASIC2 modulate responses to aversive stimuli. Genes Brain Behav. 2014; 13:179–94. [PubMed: 24256442]

RADA P, MORENO SA, TUCCI S, GONZALEZ LE, HARRISON T, CHAU DT, HOEBEL BG, HERNANDEZ L. Glutamate release in the nucleus accumbens is involved in behavioral depression during the PORSOLT swim test. Neuroscience. 2003; 119:557–65. [PubMed: 12770568]

REMPE D, VANGEISON G, HAMILTON J, LI Y, JEPSON M, FEDEROFF HJ. Synapsin I Cre transgene expression in male mice produces germline recombination in progeny. Genesis. 2006; 44:44–9. [PubMed: 16419044]

RUSSO SJ, DIETZ DM, DUMITRIU D, MORRISON JH, MALENKA RC, NESTLER EJ. The addicted synapse: mechanisms of synaptic and structural plasticity in nucleus accumbens. Trends Neurosci. 2010; 33:267–76. [PubMed: 20207024]

TAUGHER RJ, GHOBBEH A, SOWERS LP, FAN R, WEMMIE JA. ASIC1A in the bed nucleus of the stria terminalis mediates TMT-evoked freezing. Front Neurosci. 2015; 9:239. [PubMed: 26257596]

TAUGHER RJ, LU Y, WANG Y, KREPLE CJ, GHOBBEH A, FAN R, SOWERS LP, WEMMIE JA. The bed nucleus of the stria terminalis is critical for anxiety-related behavior evoked by CO2 and acidosis. J Neurosci. 2014; 34:10247–55. [PubMed: 25080586]

WALDMANN R, CHAMPIGNY G, BASSILANA F, HEURTEAUX C, LAZDUNSKI M. A proton-gated cation channel involved in acid-sensing. Nature. 1997; 386:173–7. [PubMed: 9062189]

WALKER AS, GOINGS GE, KIM Y, MILLER RJ, CHENN A, SZELE FG. Nestin reporter transgene labels multiple central nervous system precursor cells. Neural Plast. 2010; 2010:894374. [PubMed: 21527990]

WEMMIE J, CORYELL M, ASKWITH C, LEONARD S, SIGMUND C, WELSH M. Overexpression of acid-sensing ion channel 1a in transgenic mice increases fear-related behavior. Proc Natl Acad Sci U S A. 2004; 101:3621–3626. [PubMed: 14988500]

WEMMIE JA, ASKWITH CC, LAMANI E, CASSELL MD, FREEMAN JH JR, WELSH MJ. Acid-sensing ion channel 1 is localized in brain regions with high synaptic density and contributes to fear conditioning. J Neurosci. 2003; 23:5496–502. [PubMed: 12843249]

WEMMIE JA, CHEN J, ASKWITH CC, HRUSKA-HAGEMAN AM, PRICE MP, NOLAN BC, YODER PG, LAMANI E, HOSHI T, FREEMAN JH JR, WELSH MJ. The acid-activated ion channel ASIC contributes to synaptic plasticity, learning, and memory. Neuron. 2002; 34:463–77. [PubMed: 11988176]

WEMMIE JA, TAUGHER RJ, KREPLE CJ. Acid-sensing ion channels in pain and disease. Nat Rev Neurosci. 2013; 14:461–71. [PubMed: 23783197]

WU PY, HUANG YY, CHEN CC, HSU TT, LIN YC, WENG JY, CHIEN TC, CHENG IH, LIEN CC. Acid-Sensing Ion Channel-1a Is Not Required for Normal Hippocampal LTP and Spatial Memory. J Neurosci. 2013; 33:1828–1832. [PubMed: 23365222]

XIONG ZG, ZHU XM, CHU XP, MINAMI M, HEY J, WEI WL, MACDONALD JF, WEMMIE JA, PRICE MP, WELSH MJ, SIMON RP. Neuroprotection in ischemia: blocking calcium-permeable acid-sensing ion channels. Cell. 2004; 118:687–698. [PubMed: 15369669]

YANG F, SUN X, DING Y, MA H, YANG TO, MA Y, WEI D, LI W, XU T, JIANG W. Astrocytic Acid-Sensing Ion Channel 1a Contributes to the Development of Chronic Epileptogenesis. Sci Rep. 2016; 6:31581. [PubMed: 27526777]

ZHA XM. Acid-sensing ion channels: trafficking and synaptic function. Mol Brain. 2013; 6:1. [PubMed: 23281934]

ZHA XM, WANG R, COLLIER DM, SNYDER PM, WEMMIE JA, WELSH MJ. Oxidant regulated inter-subunit disulfide bond formation between ASIC1a subunits. Proc Natl Acad Sci U S A. 2009; 106:3573–8. [PubMed: 19218436]

ZHA XM, WEMMIE JA, GREEN SH, WELSH MJ. Acid-sensing ion channel 1a is a postsynaptic proton receptor that affects the density of dendritic spines. Proc Natl Acad Sci U S A. 2006; 103:16556–61. [PubMed: 17060608]

ZHANG GC, MAO LM, WANG JQ, CHU XP. Upregulation of acid-sensing ion channel 1 protein expression by chronic administration of cocaine in the mouse striatum in vivo. Neurosci Lett. 2009; 459:119–22. [PubMed: 19427358]

ZHU Y, ROMERO MI, GHOSH P, YE Z, CHARNAY P, RUSHING EJ, MARTH JD, PARADA LF. Ablation of NF1 function in neurons induces abnormal development of cerebral cortex and reactive gliosis in the brain. Genes Dev. 2001; 15:859–76. [PubMed: 11297510]

ZIEMANN AE, ALLEN JE, DAHDALEH NS, DREBOT II, CORYELL MW, WUNSCH AM, LYNCH CM, FARACI FM, HOWARD MA 3RD, WELSH MJ, WEMMIE JA. The amygdala is a chemosensor that detects carbon dioxide and acidosis to elicit fear behavior. Cell. 2009; 139:1012–21. [PubMed: 19945383]

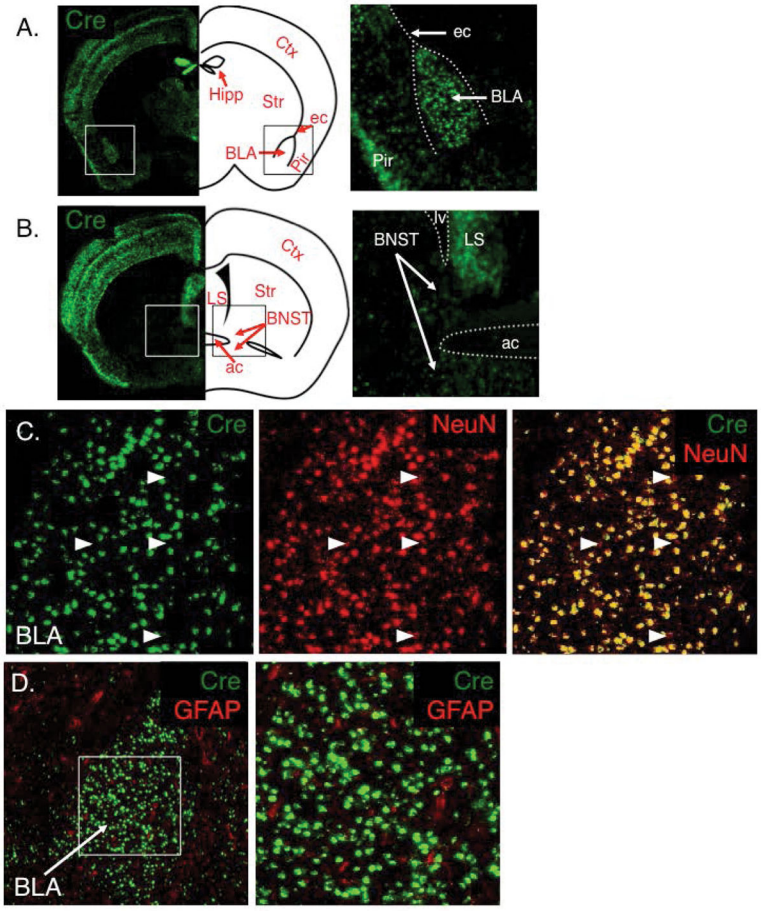

Figure 1. Cre expression is neuron-specific and widespread in *SynRosa26* mice

A, B) Coronal sections of *SynRosa26* mice showing Cre-dependent eGFP expression (green). *SynRosa26* mice expressed Cre in the BLA **(A)**. Cre was also expressed in the BNST **(B)**, although in relatively fewer cells. White squares indicate areas magnified in inset image. Anatomic structures labeled for reference include basolateral amygdala (BLA), cortex (Ctx), hippocampus (Hipp), striatum (Str), external capsule (ec), lateral ventricle (lv), piriform cortex (Pir), BNST, lateral septum (LS), and anterior commissure (ac). **C)** BLA, Cre expression (green) colocalized with NeuN (red), a marker of neuronal nuclei, although some NeuN positive cells did not express a detectable level of Cre, examples indicated by white arrowheads. **D)** In contrast, no colocalization between Cre-dependent eGFP (green) and GFAP (red), an astrocyte marker, was seen. White square indicates area magnified in inset image.

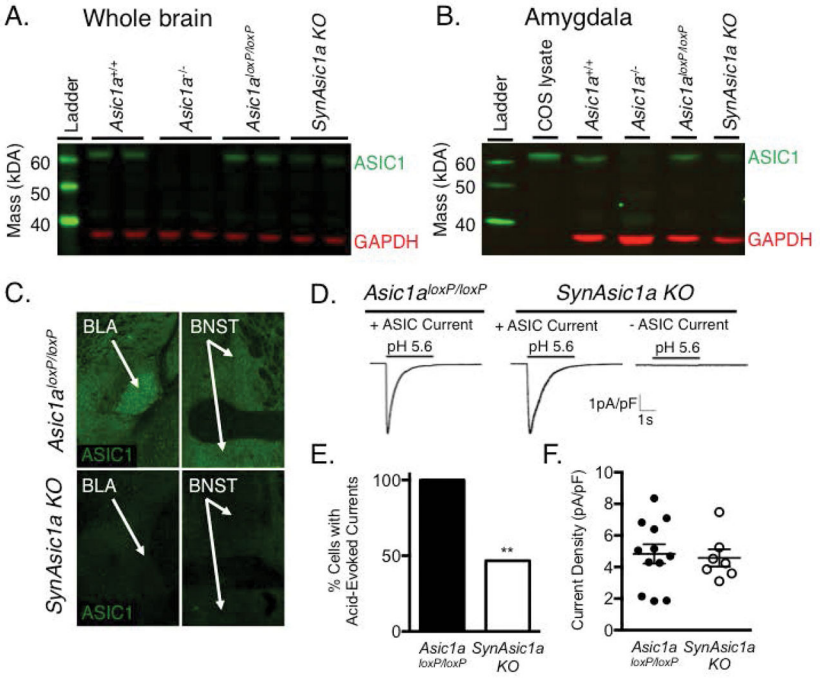

Figure 2. Disruption of ASIC1A protein in *SynAsic1a KO* mice

A, B) Western blots of protein isolated from whole brain **(A)** or amygdala punches **(B)** showing relative levels of ASIC1A expression in samples from mice of indicated genotypes. Duplicate lanes in (**A**) contained lysates from separate mice. Lysate from COS cells transfected with recombinant *Asic1a* cDNA was included as a positive control (**B**). ASIC1A (green, ~62 kDA) was detected in both whole brain and amygdala of *Asic1a*$^{+/+}$ and *Asic1a*$^{loxP/loxP}$ control mice. ASIC1A was absent in *Asic1a*$^{-/-}$ mice and reduced in *SynAsic1a KO* mice relative to Cre negative *Asic1a*$^{loxP/loxP}$ controls. GAPDH immunoblotting (red, ~37 kDa) was used to assess protein loading. **C)** ASIC1A immunohistochemistry of coronal sections taken through the BNST and BLA of *SynAsic1a KO* mice and *Asic1a*$^{loxP/loxP}$ littermates illustrating loss of ASIC1A in the *SynAsic1a KO* mice. **D–F)** Whole-cell voltage-clamp recordings of BLA neurons in slice preparation. The percentage of neurons with acid-evoked current was significantly reduced in *SynAsic1a KO* mice relative to Cre negative *Asic1a*$^{loxP/loxP}$ controls (n = 12, 15), although in neurons retaining current, the mean current density did not differ from controls.

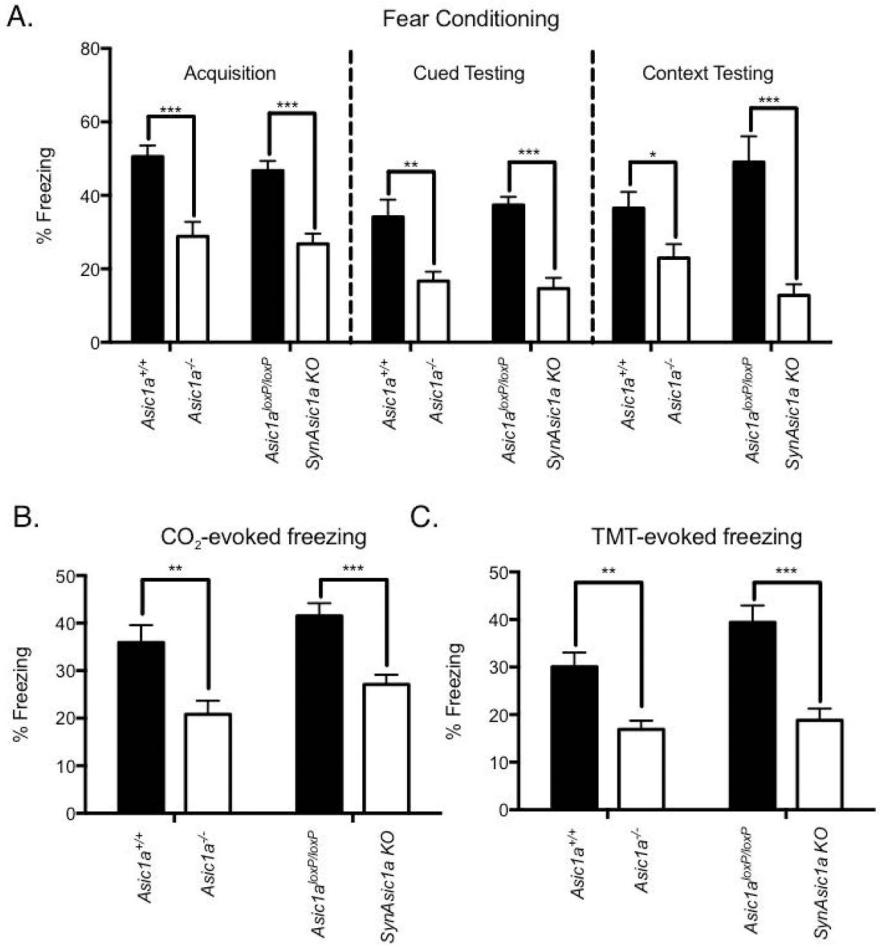

Figure 3. Conditioned and unconditioned fear-related behaviors were reduced in *SynAsic1a KO* mice

A) Compared to their respective control groups, both global *Asic1a*$^{-/-}$ mice and neuron-specific *SynAsic1a KO* mice exhibited reduced freezing during acquisition, cued testing, and context testing (n = 10, 10, 14, 17). **B)** CO_2-evoked freezing was reduced in both global *Asic1a*$^{-/-}$ mice and *SynAsic1a KO* mice (n = 11, 10, 14, 17). **C)** TMT-evoked freezing was reduced in both global *Asic1a*$^{-/-}$ mice and *SynAsic1a KO* mice (n = 10, 10, 14, 16).

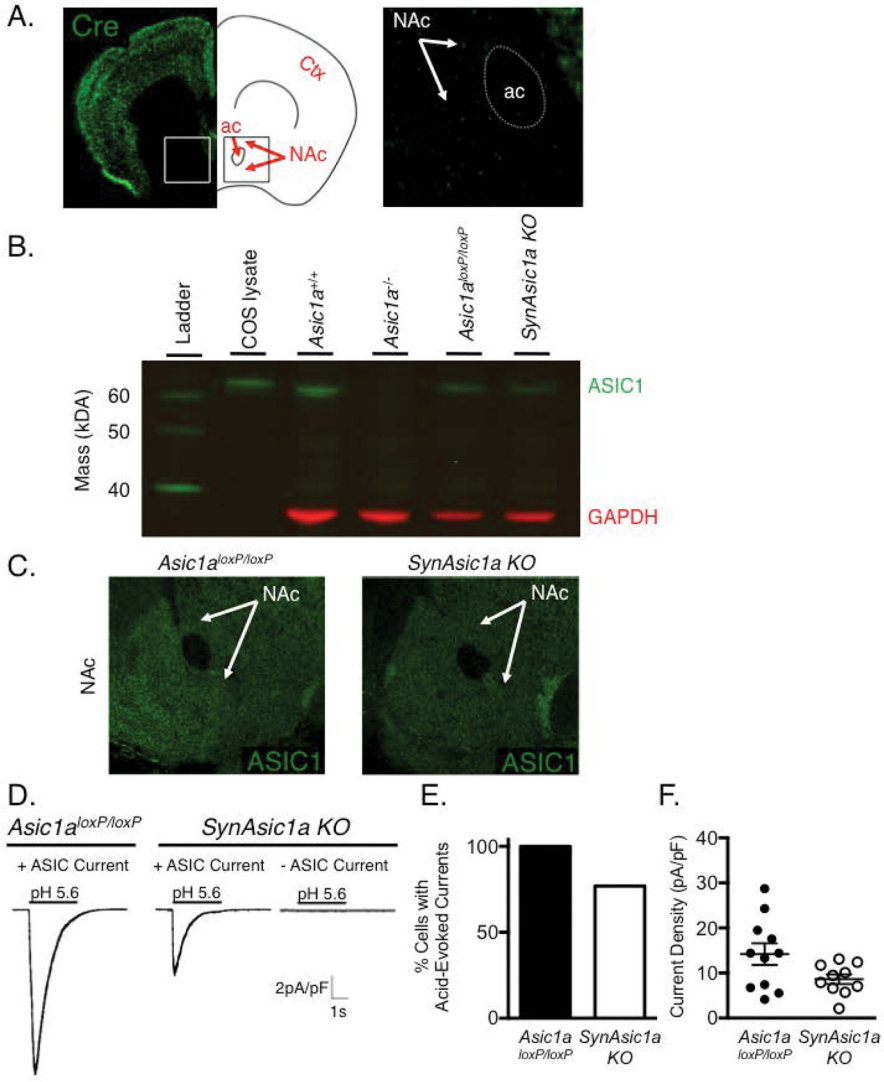

Figure 4. Preserved ASIC1A expression in the nucleus accumbens (NAc) of *SynAsic1a KO* mice

A) Coronal section through the NAc of a *SynRosa26* mouse. Although Cre-dependent eGFP expression was readily observed in cortical layers, it was rare in the NAc and striatum (Str). White square indicates magnified area including NAc (inset). Anatomic structures labeled for reference include cortex (Ctx) and anterior commissure (ac). **B)** Western blot of ASIC1A protein isolated from NAc punches of mice of the indicated genotypes, or COS cells transfected with *Asic1a* cDNA (Wemmie et al., 2002). ASIC1A (green, ~62 kDA) was detected in NAc from *Asic1a*$^{+/+}$ and *Asic1a*$^{loxP/loxP}$, and *SynAsic1a KO* mice with similar levels of ASIC1A expression in *SynAsic1a KO* mice and Cre negative *Asic1a*$^{loxP/loxP}$ controls. ASIC1A expression was absent in NAc of an *Asic1a*$^{-/-}$ mouse. GAPDH immunoblotting (red, ~37 kDa) was used to assess protein loading. **C)** ASIC1A immunohistochemistry of coronal sections through the NAc, showing similar levels of ASIC1A expression in *SynAsic1a KO* mice and *Asic1a*$^{loxP/loxP}$ controls. **D–E)** Whole-cell voltage-clamp recordings of NAc neurons in slice preparation. The majority of *SynAsic1a KO* NAc neurons exhibited acid-evoked currents and the proportion of neurons lacking acid-

evoked currents did not differ significantly from Cre negative *Asic1a*$^{loxP/loxP}$ controls (n = 11, 13). **F)** Mean acid-evoked current density in *SynAsic1a KO* cells trended lower although it did not reach statistical significance.

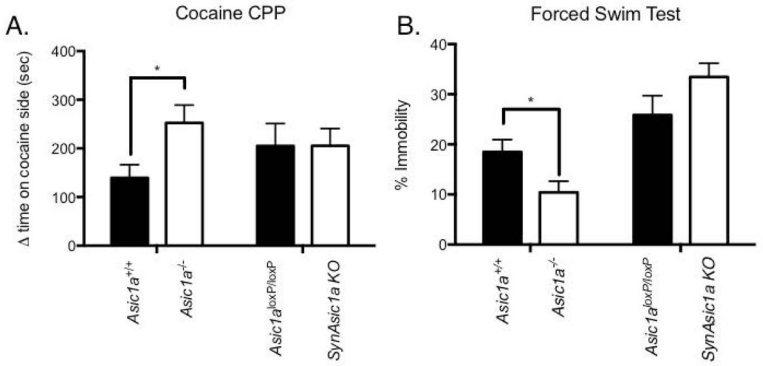

Figure 5. Some ASIC1A-dependent behaviors were intact in *SynAsic1a KO* mice

A) Relative to respective control groups, cocaine conditioned place preference (CPP) was increased by global disruption of ASIC1A in *Asic1a*$^{-/-}$ mice but not by neuron-specific disruption in *SynAsic1a KO* mice (n = 14, 14, 9, 11). **B)** Immobility in the forced swim test was reduced in global *Asic1a*$^{-/-}$ mice, but not in *SynAsic1a KO* mice (n = 10, 10, 14, 17).